Cement & Concrete Composites 33 (2011) 116–123

Contents lists available at ScienceDirect

Cement & Concrete Composites

journal homepage: www.elsevier.com/locate/cemconcomp

Detecting the time and location of cracks using electrically conductive surfaces

Mohammad Pour-Ghaz *, Jason Weiss

School of Civil Engineering, Purdue University, West Lafayette, IN 47907, USA

ARTICLE INFO

Article history:
Received 31 January 2010
Received in revised form 25 August 2010
Accepted 19 September 2010
Available online 29 September 2010

Keywords:
Conductive surface
Cracking
Crack detection
Damage detection
Electrical impedance spectroscopy
Equivalent circuit model
Health monitoring
Restrained shrinkage cracking

ABSTRACT

This paper describes the use of electrical impedance spectroscopy to detect the time, location, and approximate number of cracks on the surface of concrete. This method uses an electrically conductive thin film that is applied to the surface of the cementitious materials. The electrical resistance of this film is monitored as the substrate cracks. A sudden increase in the electrical resistance of the film corresponds with the time of cracking. The location of the cracks can be obtained when the conductive film is applied to two parallel surfaces of the cementitious material using the ratio of the capacitances (or resistances) before and after cracking. For monitoring damage evolution consisting of multiple cracks an equivalent circuit model is proposed. Using this model an increase in the electrical resistance that occurs due to the growth of a single crack can be differentiated from the increase in the electrical resistance that occurs due to the formation of more than one crack.

© 2010 Elsevier Ltd. All rights reserved.

1. Introduction

The electrical properties of cement based composites have been studied by many researchers to monitor crack development and to characterize damage [1–9]. Both direct current (DC) and alternating current (AC) has been used for these purposes. While DC resistance measurement methods are inexpensive and easy to implement and interpret, these methods can result in polarization of electrodes which hinders accurate measurements [10,11]. An alternative to the DC current measurements is the application of a low voltage alternating current using electrical impedance spectroscopy (EIS) [1,2,9,12]. Previously, EIS has been successfully applied for damage characterization and quantifying the cracking and micro-cracking in concrete and carbon fiber reinforced cement paste [1,2,7,9,13,14].

This paper introduces a method for determining the time of cracking using a thin layer of conductive material that is applied to the surface of cement based materials. The resistance of the conductive surface materials is monitored during the cracking of the substrate. When the substrate cracks the resistance of the conductive surface material increases and the time of cracking of the substrate can be captured. By using an appropriate capacitance theory a relationship between the location of the crack (distance from an electrode) and the ratio of the capacitance before and after cracking (similarly, the ratio of the resistance before and after cracking) can be established. An equivalent circuit model for conductive surfaces is introduced. The equivalent circuit model facilitates monitoring damage evolution. Using this model the resistance increase that occurs due to the growth of a single crack can be differentiated from resistance increase that occurs due to increase in the number of cracks.

2. Background

The frequency dependent response of a material that is subjected to an AC stimulus can be presented using complex electrical impedance through a Nyquist (also referred to as Cole–Cole plot) (Fig. 1a) and Bode (Fig. 1b) plot. The plot of the imaginary portion of the impedance against the real portion of the impedance is referred to as Nyquist plot. The real impedance that is measured when the imaginary portion approaches zero at different frequencies corresponds to the electrical resistance of the material [10,15–19]. For example, for the circuit shown in the insert of Fig. 1a, the electrical resistance of the circuit at low frequencies equals to the sum of all resistances of all resistors in the circuit (i.e., 95 kΩ), while the electrical resistance at cusp corresponds to the sum resistances of two smaller resistors (i.e., 13.4 kΩ). At low frequencies none of the capacitors in the circuit pass electrical current and hence the low frequency resistance of the circuit equals to the total resistance of the circuit. At higher frequencies (i.e., frequency of the cusp), however, the large capacitor in the circuit (i.e., 22 μF) passes the current and short circuits the large resistor in the circuit (i.e.,

* Corresponding author. Address: 550 Stadium Mall Drive, West Lafayette, IN 47907, USA. Tel.: +1 756 543 6201.
E-mail address: pourghaz@purdue.edu (M. Pour-Ghaz).

0958-9465/$ - see front matter © 2010 Elsevier Ltd. All rights reserved.
doi:10.1016/j.cemconcomp.2010.09.015

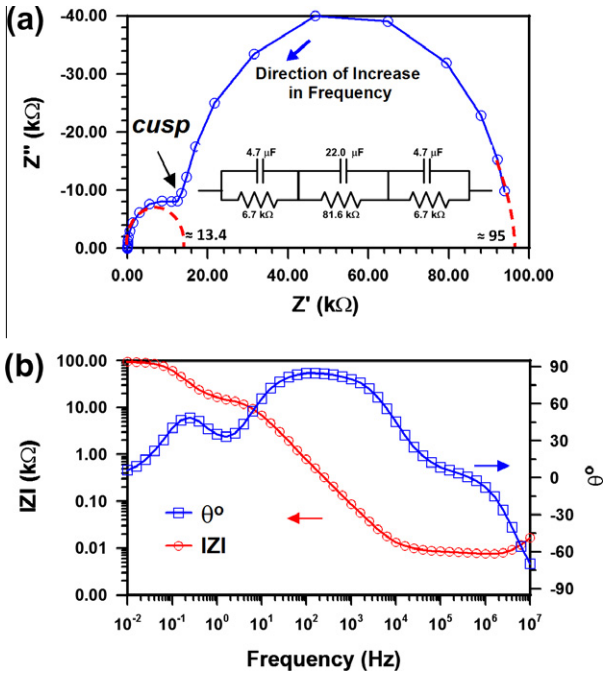

Fig. 1. (a) Nyquist plot and (b) Bode plot of the electrical circuit shown in the insert.

81.6 kΩ) and the high frequency resistance of the circuit equals to the sum of resistances of the smaller resistors in the circuit. Impedance can also be represented using the impedance (real, imaginary or total) as a function of frequency using a Bode plot [10,12,15–20]. The value of the equivalent resistance and capacitance of the material can be obtained from Nyquist and Bode diagrams [19,21–23]. Conversely, the material can be represented by an equivalent circuit that produces the same frequency dependent response.

3. Overview of the proposed method

To detect damage, conductive materials are applied to the surface of the concrete. Conductive materials such as gels, paints, and epoxy could be used for this purpose. This work used conductive colloidal silver paint and conductive copper tape. These are low cost materials that can easily and rapidly be applied to the surface of the concrete. As cracking occurs in the cement based substrate, the conductive surface material stretches and cracks causing the resistance of the conductive surface to increase. Fig. 2 provides a schematic illustration of a typical configuration for the applied paint or tape.

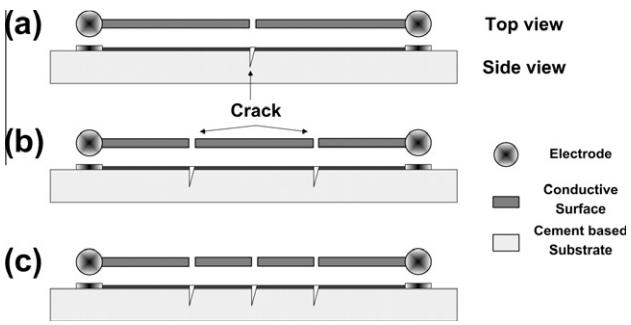

Fig. 2. Schematic illustration of a cracked conductive surface on a cement based substrate: (a) single crack, (b) two cracks, and (c) multiple cracks.

The first crack in the conductive surface can be captured by a sudden increase of the electrical resistance where the conductive surface cracks (Fig. 2a). In the case of a single crack, the part of the conductive surface material that is connected to the electrodes effectively become a part of the electrodes due to the low resistance of the conductive surface material compared to the resistance of the substrate materials (i.e., electrodes and conductive surface materials are similar in conductivity). This enables the resistance of the material across the crack (connected portion of the volume across the crack) to be measured. This is illustrated schematically in Fig. 2a. Here it is assumed that the current flows through the connected volume of the substrate after cracking. In the cases when through-cracking takes place (no connecting volume exists across the crack), the resistance of the conductive surface increases to that of the open circuit.

In the case of multiple cracking (Fig. 2b and 2c), material in between the electrodes (or the material in between the pieces of the conductive surface materials that are connected to the electrodes) consists of two distinct phases. One phase consists of highly conductive material (i.e., conductive surface) and the other phase consists of material with lower conductivity (i.e., a crack or concrete).

While the equivalent circuit model for a single crack (Fig. 2a) is similar to the equivalent circuit model for concrete (Fig. 3a) [15,16,19] the equivalent circuit model for multiple cracks (Fig. 2b and 2c) is similar to the equivalent circuit model of fiber reinforced concrete with conductive fibers (Fig. 3b) [7,18,22,24]. The conductive materials between the electrodes conduct current at relatively high frequencies and are effectively non-conductive at low frequencies [7,15,16,18,19,22,24]. The equivalent circuit models for concrete and the equivalent circuit switch model for fiber reinforced concrete are shown in Fig. 3 [7,15,16,18,19,22,24].

An increase in the number of cracks from 1 to 2 (or more) changes the equivalent circuit model of the system from Fig. 3a to Fig. 3b. With a further increase in the number of cracks (e.g., an increase from 2 to 3 cracks in Fig. 2) the low frequency resistance does not change while the high frequency resistance of the system increases. Therefore, by monitoring the evolution of the equivalent circuit model and change in high and low frequency resistance of the conductive material applied to the surface of concrete in addition to the time of cracking the damage evolution can be monitored (i.e., the resistance increase that occurs due to the growth of a single crack can be differentiated from resistance increase that occurs due to increase in the number of cracks).

In addition to detecting the time of cracking and damage evolution, conductive surface coatings can be used to detect the location of the damage; this can be done using two methods. In the first

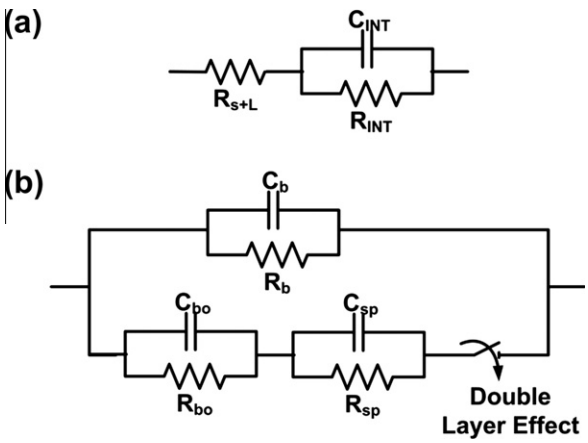

Fig. 3. (a) Equivalent circuit model for concrete [15,16,19] and (b) equivalent circuit model for fiber reinforced cement paste [18,24].

method, the conductive surface materials are applied in small segments and the resistance of each segment is monitored separately as shown in Fig. 4a. The resolution of this method for detecting the location of the cracks is dependent on the length of the segments. This method requires electrical resistance measurements between each of the two ends of each conductive surface segment. The segmental application of conductive surface coatings along with a low cost resistance measurement system [25] has several potential applications. For example one could consider a heavily restrained concrete element. The high degree of restraint causes the concrete element to be more susceptible to cracking and this method can be used to detect the time and location of cracking. Furthermore, this method can be used where the concrete element is susceptible to multiple cracking such as concrete pipelines [26].

The second method that can be used to detect the location of damage is by applying the conductive surface coatings to two parallel sides of materials as shown schematically in Fig. 4b (a sandwich structure). An experimental sample is shown in Fig. 4c. In Fig. 4b, the resistance and capacitance of the material between the two conductive surfaces is measured before and after cracking. The resistance and capacitance are related to resistivity and permittivity using [10]:

$$R = \rho \frac{d}{A} \tag{1}$$

$$C = \varepsilon \frac{A}{d} \tag{2}$$

where ρ (Ω m) is the resistivity of the cementitious material, C (F) is the capacitance, ε (F/m) is the permittivity, A (m^2) is the area of the electrode and d (m) is the distance between the electrodes (or thickness of the material). By measuring the impedance between the two surfaces (e.g., between electrodes 1 and 3 in Fig. 4b) before and after cracking and using Eqs. (1) and (2), the following equations are obtained

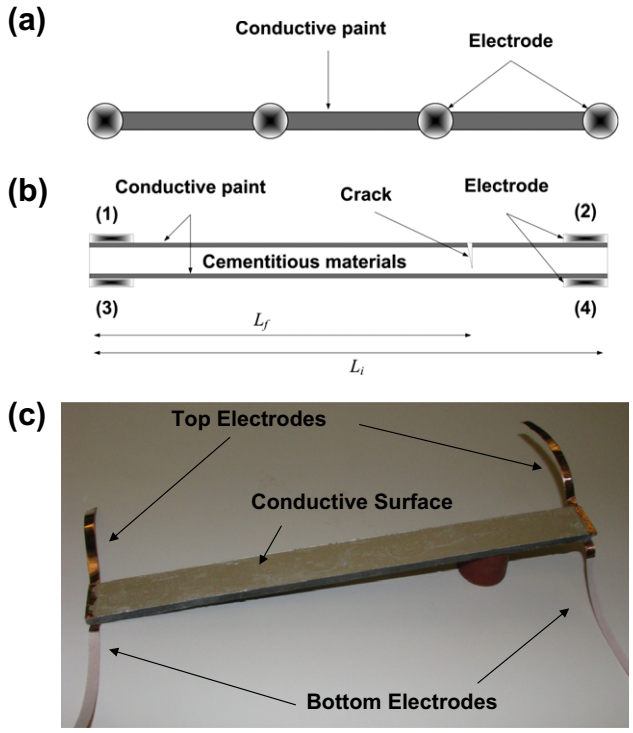

Fig. 4. (a) Schematic illustration of conductive surface segments to capture the location of the cracks, (b) conductive surfaces applied to two parallel surfaces of cement based material to capture the location of the cracks (side view) and (c) beam sample coated with conductive colloidal silver.

$$\frac{R_i}{R_f} = \frac{L_f}{L_i} \tag{3}$$

$$\frac{C_i}{C_f} = \frac{L_i}{L_f} \tag{4}$$

where subscripts i and f refer to initial (before cracking) and final (after cracking) and L_i is the length of the conductive surface coating. Using Eqs. (3) and (4) the location of the crack (L_f) measured from a reference location can be obtained.

More information on subsequent cracking of the substrate material for the geometry given in Fig. 4b can be extracted by electrical resistance measurement between different electrodes shown in Fig. 4b. If more than one crack occurs measurements between electrodes 1 and 3 (or 4), 2 and 4 (or 3) and finally 1 and 2 can provide the necessary information for determining the location and number of cracks.

4. Experimental procedure

4.1. Detecting the time of cracking in restrained shrinkage specimens

To evaluate the use of conductive surface materials and EIS for determining the time of cracking, the restrained ring [12,27–30] and restrained base [12] (corrugated steel base) test methods are used to restrain the concrete and induce stresses that cause cracking.

The restrained ring method consists of casting an annulus cementitious material around a steel ring. The steel ring resists the volume change due to shrinkage causing stress development in the cementitious material which can result in cracking [12,27,29]. The strain development in the steel ring is monitored and compared with the electrical method (resistance change in conductive paint or conductive tape applied to the surface of the cementitious materials). The development of strain in the steel ring is a function thickness of the steel ring (degree of restraint that steel ring provides). With increase of thickness of the steel ring (i.e., increase of degree of restraint) the strain that develops in the steel decreases [27–29]. For steel rings with large thickness detecting the time of cracking using strain gages becomes more difficult. The geometry of the ring used in the present work in chosen so that the developed strain can be easily monitored using strain gages to prove the concept.

The restrained base experiment [12] consists of a cementitious materials cast on top of a corrugated steel bar. Due to restraining effect of the steel and shrinkage of the cementitious material cracking may occur which is captured using conductive surface coatings at the surface. Fig. 5a schematically illustrates the sample geometries used for both restrained ring and restrained base method. It is noted that to detect the time of cracking of the ring samples two conductive surface materials were used: colloid silver paint and conductive copper tape. Copper electrodes were mounted on the samples to connect the conductive coatings to wires. Two electrode arrangements were considered for the restrained ring test. In the first arrangement two electrodes were installed at 180° with respect to each other and conductive surface materials were applied to connect these two electrodes in both directions. This arrangement is referred to as two-directional electrode arrangement. In the second electrode arrangement, electrodes were mounted 2 cm apart and conductive materials were applied to connect the electrodes in the longer path (approximately 360°). This arrangement is referred to as one-directional electrode arrangement. Fig. 6a illustrates the one-directional (Fig. 6a and c) and two-directional (Fig. 6b and d) electrode arrangements.

Silver paint was used in both electrode arrangements; however, copper tape was only used in the one-directional arrangement. The

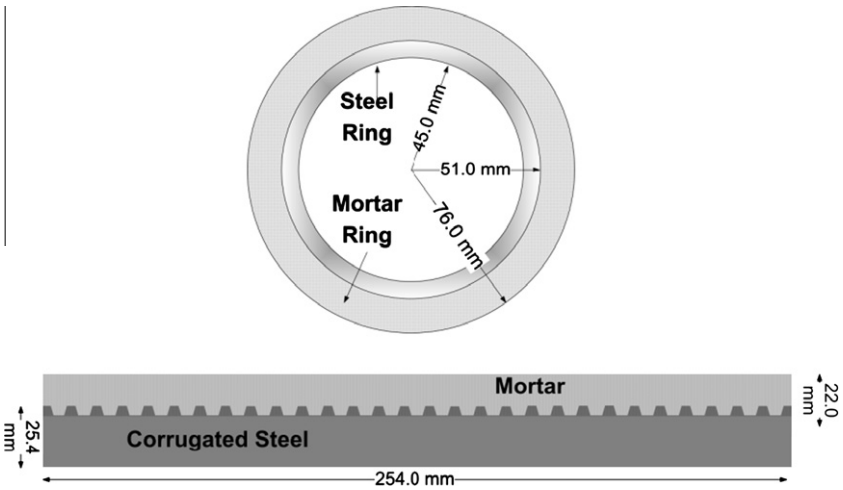

Fig. 5. Schematic illustration of restrained ring and restrained base sample (corrugated steel base) geometries.

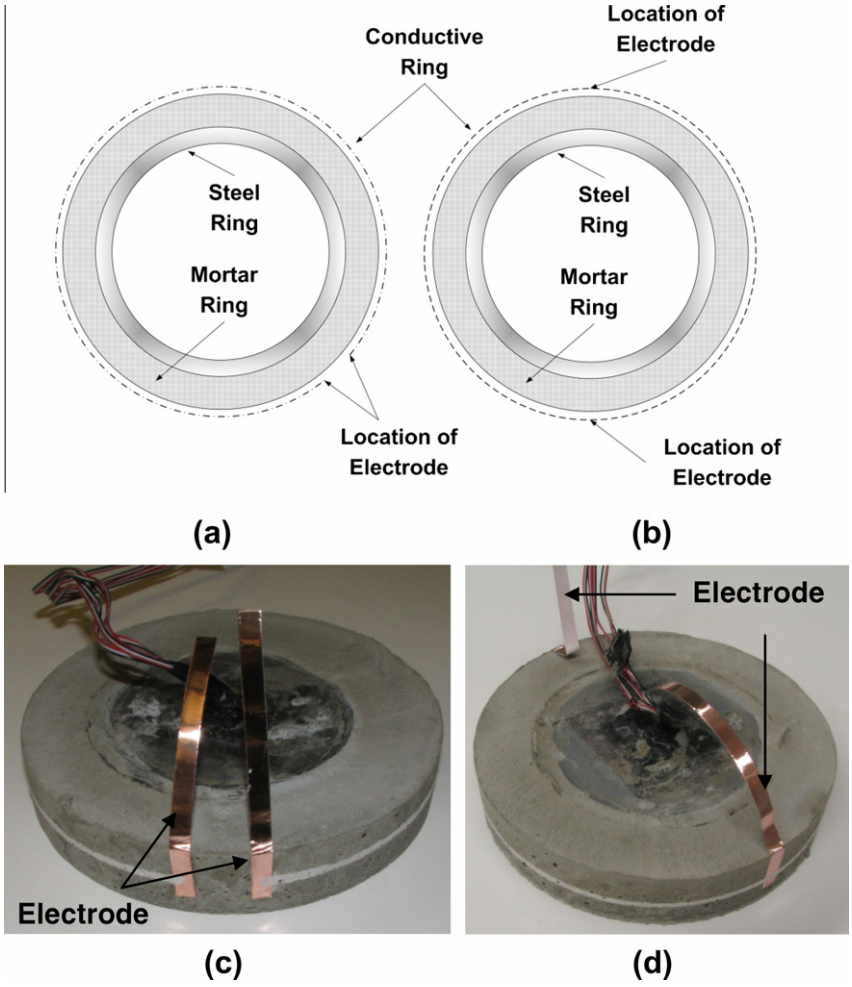

Fig. 6. Location of electrodes for: (a) one-directional and (b) two-directional electrode arrangements, (c) sample with one-directional and (d) sample with two-directional electrode arrangement (before sealing).

difference between these two electrode arrangements is that in the one-directional arrangement, after the first cracking there is no electrical connection through the conductive surface between the two electrodes while in the two-directional electrode arrangement, the electrodes remain connected through a conductive path in the second direction after the first cracking. This difference influences the magnitude of resistance change after cracking and the interpretation of resistance change.

Two mortar compositions (plain and steel fiber reinforced) were used in the restrained ring experiments. Plain mortar was produced using ordinary portland cement (OPC) with a water-to-cement ratio (w/c) of 0.30, 25% fine aggregate volume, and 0.5% high range water reducer by weight of cement. A low aggregate volume was used to induce shrinkage cracking in a short time after the exposure to drying. The steel fiber reinforced mortars consist of the same mixture proportions with addition of 1% steel fibers by volume. The steel fibers were 25 mm long and 0.60 mm in diameter. Mixing was performed in a small Hobart mixer according to ASTM C 305 for the plain mortar and for the fiber reinforced mortars this mixing was followed by additional 5 min mixing by hand after the fibers were added.

The ring samples were de-molded 24 h after casting and conductive surface coating were applied. The width of the silver paint was approximately 2 mm and width of the copper tape was approximately 1.5 mm in all experiments. The ring samples were exposed to 50 ± 1% relative humidity (RH) at 23 ± 0.5 °C after de-molding.

To determine the time of cracking in the restrained base experiment (corrugated steel) cement paste with w/c of 0.3 were cast on top of the corrugated steel. Cement paste with low w/c exposed to low relative humidity was chosen in this experiment to facilitate visual examination to confirm the time of cracking. The samples were de-molded 24 h after casting and conductive silver paint was applied to the surface of the paste. The width of the silver coating was 2 mm. Samples were exposed to 30 ± 1% RH at 23 ± 0.5 °C. In addition to electrical measurements samples were examined visually approximately every 30 min.

4.2. Parallel electrode setup for determining the location of damage

To determine the location of cracking using the parallel surface method, cement paste beams of 30 × 2.5 × 0.5 cm with w/c of 0.5 were prepared. The geometry of the sample is schematically illustrated in Fig. 4b and the sample is shown in Fig. 4c. The cement paste beams were de-molded after 24 h and cured for 48 h at 100% RH. The experiment was performed on both saturated and oven-dried samples to investigate the effect of moisture content on accuracy of this method. In case of saturated beam samples, after application of the silver paint to both surfaces of the beam (30 × 2.5 cm surface), the beams were vacuum saturated for 4 h, and in the case of oven-dried beam samples, the samples were stored at 105 ± 1 °C for 24 h before application of the paint. One hour of drying was considered after application of paint to the oven-dried samples during which the samples were placed in an air-tight container.

In this experiment cracks were simulated. To simulate the cracks, the paint was cut approximately 2 mm deep and 0.1 mm wide on one of the surfaces. The cracks were created perpendicular to the 30 × 2.5 cm face of the beam. The electrical conductivity across the crack was examined before the EIS measurements to ensure no short circuit exists.

5. Results and discussion

5.1. Using restrained shrinkage method for detecting time of cracking

Fig. 7 illustrates experimental results from a restrained ring test using plain mortar. Conductive silver paint with one-directional electrode arrangement was used in this experiment. Fig. 7 shows the strain that is measured in the inner surface of the steel ring and the electrical resistance of the conductive silver. The resistance measurements are obtained at 20 min intervals after de-molding the sample at 24 h. By exposure of the sample to drying, stress

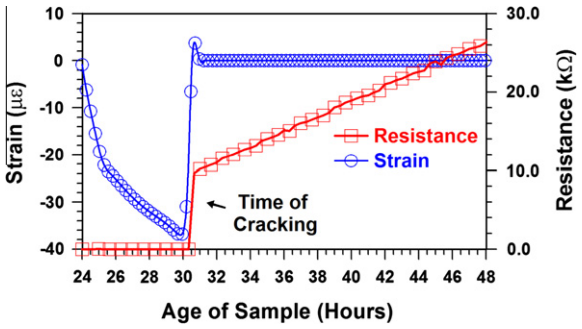

Fig. 7. Time of cracking detected by monitoring the strain at the inner surface of the steel ring and resistance of the silver paint (one-directional electrode arrangement) applied to the surface of mortar.

(measured using strain on the steel ring [12,27–29]) develops in the mortar. The time of cracking in plain mortar is detected by a sudden release of the strain in the steel ring. This strain release corresponds to the time of cracking detected by monitoring the resistance of the conductive surface paint (i.e., increase in the electrical resistance of the conductive paint). The resistance of the conductive surface increases steadily after cracking while the strain values remains nearly zero. This increase in the resistance after cracking can be attributed to two effects: opening of the crack due to the continuous drying, and drying of the sample resulting in an increase in the resistance of the mortar.

Fig. 8, illustrates the experimental results for the restrained ring test using plain mortar. Conductive silver paint with two-directional electrode arrangement was used in this experiment. Similar to Fig. 7 the time of cracking is captured by a sudden increase of the resistance of the conductive surface coating.

The resistance increase due to cracking in Fig. 7 is several orders of magnitude larger than the resistance increase in Fig. 8. This is due to the fact that a conductive path still exists between the electrodes even after cracking (in the two-directional electrode arrangement). In the one-directional electrode arrangement no conductive path remains between the two electrodes after cracking. Unlike Fig. 7 in Fig. 8, the resistance of the paint does not continue to increase after the change at cracking. In Fig. 8, the initial decrease of the resistance is the effect of the drying/aging of the colloidal silver paint. A portion of this decrease in resistance is due to shrinkage of the substrate. The decrease in the resistance is observed also after cracking. This decrease in resistance is also the effect of drying/aging of the colloidal silver paint (and shrinkage of substrate) since in two-directional arrangement a conductive path still exists between the electrodes after cracking and current flows through this path preferentially.

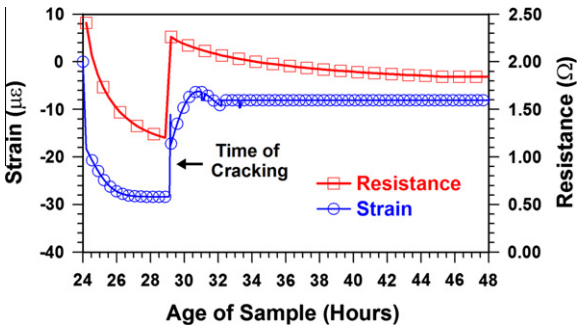

Fig. 8. Time of cracking detected by monitoring the strain a steel ring and the resistance increase of the silver paint (two-directional electrode arrangement) applied to the surface of mortar.

Fig. 9 illustrates the strain that is measured on the inner surface of the steel ring and the resistance of a conductive copper tape applied to the surface of the mortar. The time of cracking corresponds with the strain release. A non-conductive adhesive was used to mount the copper tape on the mortar to avoid slippage and/or peeling during the cracking. This adhesive prevents the passage of the current from the tape to the mortar and therefore the effect of crack opening and drying after cracking is not captured.

Plain mortar (which was used in the experiments described) results in localization of the damage in one location and a single crack in the restrained ring test. The addition of fibers, on the other hand, results in stress transfer across the cracks. This stress transfer can result in a smaller crack width and multiple cracks.

Fig. 10, illustrates the results of the restrained ring test for a steel fiber reinforced mortar. In this experiment conductive silver paint was applied to the surface of the mortar in a one-directional electrode arrangement. Two cracks are detected by both strain measurements and electrical resistance measurements of the conductive surface.

The first crack is detected by the electrical resistance measurements at the time of the first strain release in the steel ring; however, there is a time lag in detecting the second crack with the electrical resistance measurements. This observation can be explained as follows. After the first crack is developed, the residual stress in the mortar decreases significantly (strain decreases in the steel ring), therefore the second crack opens slowly at the surface of the mortar. This causes a time lag in capturing the time of the second crack using the electrical measurements since the crack is not wide enough initially to rupture the paint. The resistance increase due to the second crack is smaller compared to the resistance increase due to the second crack.

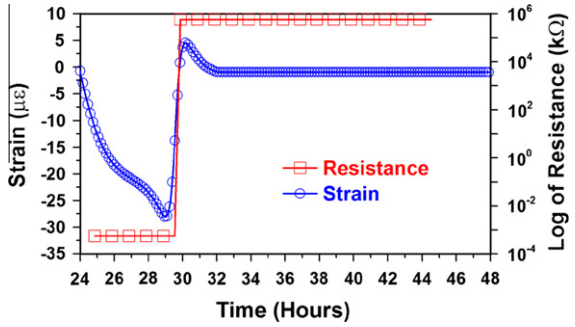

Fig. 9. Time of cracking detected by monitoring the strain at the inner surface of the steel ring and resistance of copper tape applied to the surface of mortar in restrained ring test.

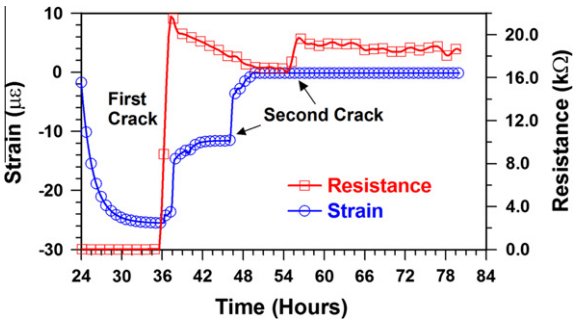

Fig. 10. Time of cracking detected by monitoring the strain at the inner surface of the steel ring and resistance of silver paint (one-directional electrode arrangement) applied to the surface of steel fiber reinforced mortar.

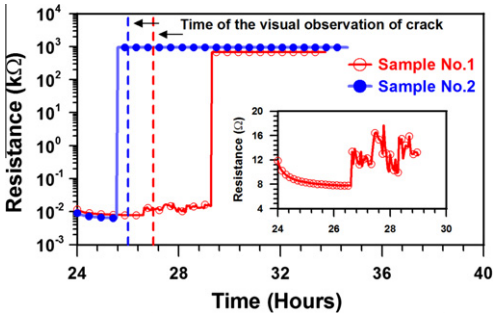

Fig. 11. Time of cracking detected using resistance measurements of conductive surface coating applied to the surface of cement paste samples ($w/c = 0.3$) and visual examination on restrained base experiment; insert illustrates closer view of the results of sample No. 1 at the time of cracking.

Fig. 11 illustrates the results of the resistance measurements of the conductive silver paint on the surface of cement paste in a restrained base experiment for two samples. Dashed lines in Fig. 11 shows the time at which the cracks on the surface were visually observed. Cracks were observed at the first visual inspections after cracking on both samples.

The resistance increase at the time of cracking is significantly larger for sample No. 2 compared to sample No. 1; however, the time of cracking of both samples is close to each other. The insert in Fig. 11 illustrates the resistance increase of the sample No. 1 at the time of cracking. Many factors such as crack width, quality of the paint at the location of the crack, thickness of the paint and the quality of the surface finish can affect the resistance change at the time of cracking. Further work is currently ongoing to accurately determine the resolution of this method in detecting the cracks. Improvement in the method of application of the paint to ensure consistency is required to minimize this effect.

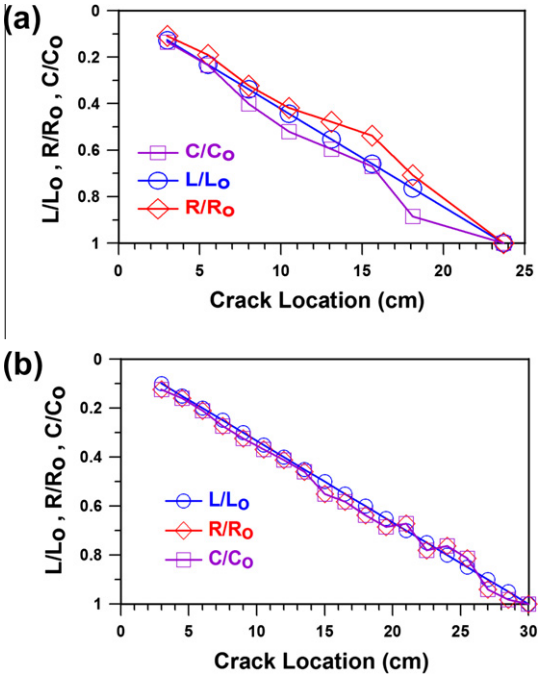

Fig. 12. Ratio of resistances and capacitances before and after cracking compared to measured ratio of distance of crack to the initial length L_f/L_i for: (a) water saturated cement paste sample and (b) oven-dried cement paste sample.

5.2. Parallel electrode setup for determining the location and number of cracks

Eqs. (3) and (4) show that the ratio of the capacitances (or electrical resistances) before and after cracking are equal to the ratio of the distance of the crack measured from an electrode to the initial length of the electrode. For example in Fig. 4b, if the resistance (or capacitance) of the sample is measured between electrode Nos. 1 and 3 before and after cracking, Eqs. (3) and (4) can be used to obtain the distance of the crack from electrode No. 3 (i.e., L_f).

Fig. 12a illustrates experimentally measured ratios of C_i/C_f, R_i/R_f and L_f/L_i for the water saturated cement paste beams And Fig. 12b illustrates these results for the oven-dried samples. The geometry of the sample and electrode arrangements are shown in Fig. 4c. The resistance and capacitance ratios in Fig. 12a and 12b are close to the actual length ratios. Therefore when L_f is an unknown, it can be calculated from C_i/C_f, R_i/R_f using Eqs. (3) and (4) accurately.

For the sample geometry shown in Fig. 4b, the location of the first crack can be obtained by measuring the impedance between electrodes 1 and 3 (or 1 and 4) (as shown in Fig. 12) and the location of the second crack can be detected by subsequent measurements between electrodes 2 and 4 (or electrodes 2 and 3). Further cracking can be captured by the resistance measurement between electrodes 1 and 2.

6. Conclusion

A method is presented in this paper that can be used to detect the time and location of cracking. The method consists of applying conductive materials to the surface of concrete or other cementitious materials and monitoring the resistance of the conductive surface coating material as the concrete substrate undergoes cracking. This method is applicable to samples with large dimensions. This can include large concrete slabs or concrete pipelines as it is a "low cost sensor." Examples of application of this method were shown where this method was applied to restrained ring test. This method can also be expanded to a wide range of geometries.

In addition to being able to detect the crack location, the approximate number of cracks in the material can be determined using different arrangements of electrodes and application of conductive surface materials.

A frequency bifurcation model is introduced for a conductive surface undergoing cracking. This equivalent model circuit can be used to monitor damage evolution. The equivalent circuit model facilitates differentiation between increase in resistance of conductive surface due to increase in crack width of a single crack and increase in resistance due to multiple cracking.

The time of cracking, in the restrained ring test using conductive surface materials was captured accurately when cracking occurs in one location, however, the width of the crack that develops may influence the accuracy of the time of cracking. In this work the smallest crack width detected was 0.05 mm. Further investigation is currently ongoing to determine the accuracy and resolution of crack detection using this method. The proposed method can capture number of cracks accurately up to three cracks in linear geometry and resolution decreases with increase of number of cracks.

Acknowledgments

This work was conducted in the Pankow Materials Laboratory and the Materials Sensing and Characterization Laboratory at Purdue University. The authors would like to acknowledge the support which has made these laboratories and this research possible.

This work is supported in part by the National Science Foundation under the NEES Program (Grant CMMI-0724022) which is greatly acknowledged. Any opinions, findings, and conclusions or recommendations expressed in this material are those of the author(s) and do not necessarily reflect the views of the National Science Foundation.

References

[1] Gu P, Xie P, Beaudoin JJ. Impedance characterization of microcracking behavior in fiber-reinforced cement composites. Cem Concr Compos 1993;15(3):173–80.
[2] Gu P, Xu Z, Xie P, Beaudoin JJ. An AC impedance spectroscopy study of microcracking in cement-based composites during compressive loading. Cem Concr Res 1993;23(3):675–82.
[3] Chen PW, Chung DLL. Carbon-fiber-reinforced concrete as an intrinsically smart concrete for damage assessment during dynamic loading. J Am Ceram Soc 1995;78(3):816–8.
[4] Chen PW, Chung DLL. Concrete as a new strain/stress sensor. Compos Part B: Eng 1996;27(1):11–23.
[5] Chen PW, Chung DLL. Carbon-fiber-reinforced concrete smart structures capable of nondestructive flaw detection. In: Proceedings of SPIE – the international society for optical engineering, vol. 1916; 1993. p. 445–53.
[6] Bontea DM, Chung DDL, Lee GC. Damage in carbon fiber-reinforced concrete, monitored by electrical resistance measurement. Cem Concr Res 2000;30(4):651–9.
[7] Peled A, Torrents JM, Mason TO, Shah SP, Garboczi EJ. Electrical impedance spectra to monitor damage during tensile loading of cement composites. ACI Mater J 2001;98(4):313–22.
[8] Cao J, Chung DDL. Defect dynamics and damage of concrete under repeated compression, studied by electrical resistance measurement. Cem Concr Res 2001;31(11):1639–42.
[9] Niemuth M. Using impedance spectroscopy to detect flaws in concrete. MASc thesis. West Lafayette, Purdue University; 2004.
[10] Macdonald JR, William RK. Impedance spectroscopy: emphasizing solid materials and systems. New York: Wiley-Interscience; 1987.
[11] Uhlig HH, Revie RW. Corrosion and corrosion control. New York: Wiley-Interscience; 1985.
[12] Weiss WJ. Prediction of early-age shrinkage cracking in concrete. Ph.D. thesis. Evanston, Northwestern University; 1999.
[13] Reza F, Yamamuro JA, Batson GB, Lee JS. Smart behavior of carbon fiber cement composites in compact tension. In: Proceedings of the 16th ASCE engineering mechanics conference, Seattle, University of Washington; 2003.
[14] Hou TC, Lynch JP. Electrical impedance tomographic methods for sensing strain fields and crack damage in cementitious structures. J Intell Mater Syst Struct 2009;20(11):1363–79.
[15] Christensen BJ. Microstructure studies of hydrating portland cement-based materials using impedance spectroscopy. Ph.D. thesis. Evanston, Northwestern University; 1993.
[16] Christensen BJ, Coverdale RT, Olson RA, Ford SJ, Jennings HM, Mason TO. Impedance spectroscopy of hydrating cement-based materials: measurement, interpretation, and application. J Am Ceram Soc 1994;77(11): 2789–804.
[17] Coverdale RT, Christensen BJ, Mason TO, Jennings HM, Garboczi EJ. Interpretation of the impedance spectroscopy of cement paste via computer modeling. J Mater Sci 1994;29(19):4984–92.
[18] Mason TO, Campo MA, Hixson AD, Woo LY. Impedance spectroscopy of fiber-reinforced cement composites. Cem Concr Compos 2002;24(5):457–65.
[19] Gu P, Xie P, Beaudoin JJ, Brousseau R. AC impedance spectroscopy (I): a new equivalent circuit model for hydrated portland cement paste. Cem Concr Res 1992;22(5):833–40.
[20] Rajabipour F. Insitu electrical sensing and material health monitoring in concrete structures. Ph.D. thesis. West Lafayette, Purdue University; 2006.
[21] MacPhee DE, Sinclair DC, Cormack SL. Development of an equivalent circuit model for cement pastes from microstructural considerations. J Am Ceram Soc 1997;80(11):2876–84.
[22] Torrents JM, Mason TO, Garboczi EJ. Impedance spectra of fiber-reinforced cement-based composites: a modeling approach. Cem Concr Res 2000;30(4):585–92.
[23] Woo LY, Wansom S, Hixson AD, Campo MA, Mason TO. A universal equivalent circuit model for the impedance response of composites. J Mater Sci 2003;38(10):2265–70.
[24] Hixson AD, Woo LY, Campo MA, Mason TO, Garboczi EJ. Intrinsic conductivity of short conductive fibers in composites by impedance spectroscopy. J Electroceram 2001;7(3):189–95.
[25] Poursaee A, Weiss J. Development of an automated electrical monitoring system (AEMS) to assess properties of concrete. Automat Constr 2010;19(4):485–90.
[26] Bradshaw AS, daSilva G, McCue MT, Kim J, Nadukuru, SS, Lynch J, Michalowski RL, Pour-Ghaz M, Weiss J, Green R. Damage detection and health monitoring of buried concrete pipelines. In: Oka F, Murakami A, Kimoto S, editors. Proceedings of international symposium on prediction and simulation methods for Geohazard mitigation (IS Kyoto 2009), Kyoto; 2009. p. 473–8.

[27] Hossain AB, Weiss WJ. Assessing residual stress development and stress relaxation in restrained concrete ring specimens. Cem Concr Compos 2004;26(5):531–40.
[28] Moon JH, Rajabipour F, Pease B, Weiss WJ. Quantifying the influence of specimen geometry on the results of the restrained ring test. J ASTM Int 2006;3(8).
[29] Moon JH, Weiss WJ. Estimating residual stress in the restrained ring test under circumferential drying. Cem Concr Compos 2006;28(5):486–96.
[30] Shah HR, Weiss WJ. Quantifying shrinkage cracking in fiber reinforced concrete using the ring test. Mater Struct 2006;39(293):887–99.